

On initial-value and self-similar solutions of the compressible Euler equations

Ravi Samtaney and D. I. Pullin

Graduate Aeronautical Laboratories, California Institute of Technology, Pasadena, California 91125

(Received 9 January 1996; accepted 20 May 1996)

We examine numerically the issue of convergence for initial-value solutions and similarity solutions of the compressible Euler equations in two dimensions in the presence of vortex sheets (slip lines). We consider the problem of a normal shock wave impacting an inclined density discontinuity in the presence of a solid boundary. Two solution techniques are examined: the first solves the Euler equations by a Godunov method as an initial-value problem and the second as a boundary value problem, after invoking self-similarity. Our results indicate nonconvergence of the initial-value calculation at fixed time, with increasing spatial-temporal resolution. The similarity solution appears to converge to the weak 'zero-temperature' solution of the Euler equations in the presence of the slip line. Some speculations on the geometric character of solutions of the initial-value problem are presented. © 1996 American Institute of Physics. [S1070-6631(96)02609-8]

I. INTRODUCTION

It is well known that the linear stability of a plane vortex sheet in two dimensional incompressible flow is *ill-posed*^{1,2} in the sense of Hadamard.³ The corresponding nonlinear problem was analyzed by Moore,⁴ who demonstrated derivative singularities in a finite time t_c from smooth initial conditions. As a consequence, numerical initial-value calculations of vortex sheet motion for analytic initial data converge only for $t < t_c$,² and require special techniques to control the growth of modes stimulated by roundoff error.¹ Delort⁵ proved that in the special case where the vortex sheet strength (local velocity difference) is one-signed, the incompressible Euler equations with vortex-sheet initial data have weak solutions. This does not imply that the weak solution itself has a vortex-sheet structure or that if it does, it has any particular fractal dimension, although solutions containing vortex sheets with dimension greater than unity cannot be ruled out. There remain nontrivial questions concerning uniqueness and the geometrical character of admissible solutions. There is no known general method for computing such incompressible flows for arbitrary time intervals in two or three space dimensions.

In two-dimensional compressible flow, vortex sheets or slip lines (i.e., contact discontinuities with a jump in the tangential velocity) are produced spontaneously at a triple point, or from shock diffraction over a right-angle corner, or from irregular reflection of a shock at a solid boundary. Linear stability analysis of a vortex sheet in compressible inviscid flow indicates ill-posedness if the convective Mach number (M_c) is less than unity.⁶ The existence of weak solutions of the compressible Euler equations in multidimensions is not known in general but it seems reasonable to suppose that Delort's result for the incompressible case will be valid. Whilst several authors have referred to the presence of grid-scale Kelvin–Helmholtz instability when slip-line discontinuities are present, (e.g., Quirk,⁷ Berger and Colella,⁸ etc.) little attention has been paid to questions of convergence in the presence of vortex sheets. Mulder *et al.*⁹ studied Rayleigh–Taylor and Kelvin–Helmholtz instabilities and re-

ported a lack of convergence for their inviscid computations even though they employed relatively coarse meshes. Bell *et al.*¹⁰ mention in passing convergence problems for computations of an inviscid incompressible flow with vortex-sheet initial data. In many computational studies of multidimensional compressible flow there appears to be an implicit assumption that there exists, at some fixed time, an appropriate unique weak solution of the compressible Euler equation in which the slip-line discontinuity is embedded as a rectifiable curve, and that (by analogy with the one-dimensional case) convergence to this solution with increasing grid refinement can be achieved.

In this study, we provide computational evidence which we hope will elucidate the issue of convergence with respect to grid refinement of both initial-value and similarity solutions of the compressible Euler equations, in the presence of vortex sheets. The specific flow considered is that of shock wave refraction at a gaseous interface separating gases of different acoustic impedances (see Fig. 1). We consider numerical solutions of the compressible Euler equations in conservative form,

$$U_t + F_x(U) + G_y(U) = 0, \quad (1)$$

where

$$\begin{aligned} U(x, y, t) &= \{\rho, \rho u, \rho v, E\}^T, \\ F(U) &= \{\rho u, \rho u^2 + p, \rho uv, (E + p)u\}^T, \\ G(U) &= \{\rho v, \rho uv, \rho v^2 + p, (E + p)v\}^T. \end{aligned}$$

By inspection, we note the existence of a self-similar solution in the scaled variables ($\xi \equiv x/t, \eta \equiv y/t$). Equation (1) reduces to¹¹

$$2\tilde{U} + \tilde{F}_\xi + \tilde{G}_\eta = 0, \quad (2)$$

where

$$\begin{aligned} \tilde{F} &= \{\rho(u - \xi), \rho u(u - \xi) + p, \rho(u - \xi)v, E(u - \xi) + pu\}^T, \\ \tilde{G} &= \{\rho(v - \eta), \rho u(v - \eta), \rho v(v - \eta) + p, E(v - \eta) + pv\}^T, \\ \tilde{U}(\xi, \eta) &\equiv U(x, y, t). \end{aligned}$$

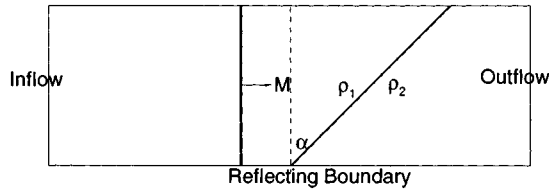


FIG. 1. Schematic of a shock interaction with a gaseous density interface. Boundary conditions are inflow/outflow in the x direction and reflecting in the y direction.

The system of equations (1) is *hyperbolic* while the system (2) is of the *mixed hyperbolic-elliptic* type. The self-similar solution is a *fixed point of the boundary value problem* given by Eq. (2).

We focus on the specific case of a Mach 2.02 shock wave refraction at a gaseous interface separating gases of density $\rho_1=1$, $\rho_2=3$, inclined at an angle of $\alpha=60^\circ$ to the plane of the shock. The interface is initially in mechanical and thermal equilibrium. The pressure in the unshocked gases is unity and the ratio of specific heats is taken to be 1.4.

II. THE INITIAL-VALUE PROBLEM

Equation (1) is solved numerically as an *initial-value problem*. We employ the Godunov method¹² extended to second order accuracy by fitting linear profiles in each cell and applying monotonicity constraints, i.e., slope limiting.¹³ The solution is marched in time until time, $t=1$. Numerical solutions were obtained for grids of sizes: (a) 768×392 (coarse, mesh spacing $\Delta x = \Delta y = h$) (b) 1536×768 (medium, $\Delta x = h/2$) and (c) 3072×1536 (fine $\Delta x = h/4$). Gray scale density images are displayed in Fig. 2. The shock refractions leads to a transmitted and a reflected shock. The transmitted shock culminates as a Mach stem at the lower boundary. Owing to the baroclinic source term (i.e., a misalignment of density and pressure gradients) circulation is generated on the shocked interface which produces a slip-line discontinuity for which the convective Mach number $M_c \approx 0.3$.¹⁴ It is therefore locally *linearly unstable*. There is roll-up at the lower boundary. The remaining portion of the shear layer appears to be smooth for the coarse grid. Comparison of the density images of Fig. 2 shows increasing complexity of the contours in the vicinity of the slip line, from the coarse to the fine grid. As the grid is refined, there is clearly no pointwise convergence in this region, which itself shows no evidence of reducing in area; in fact we see

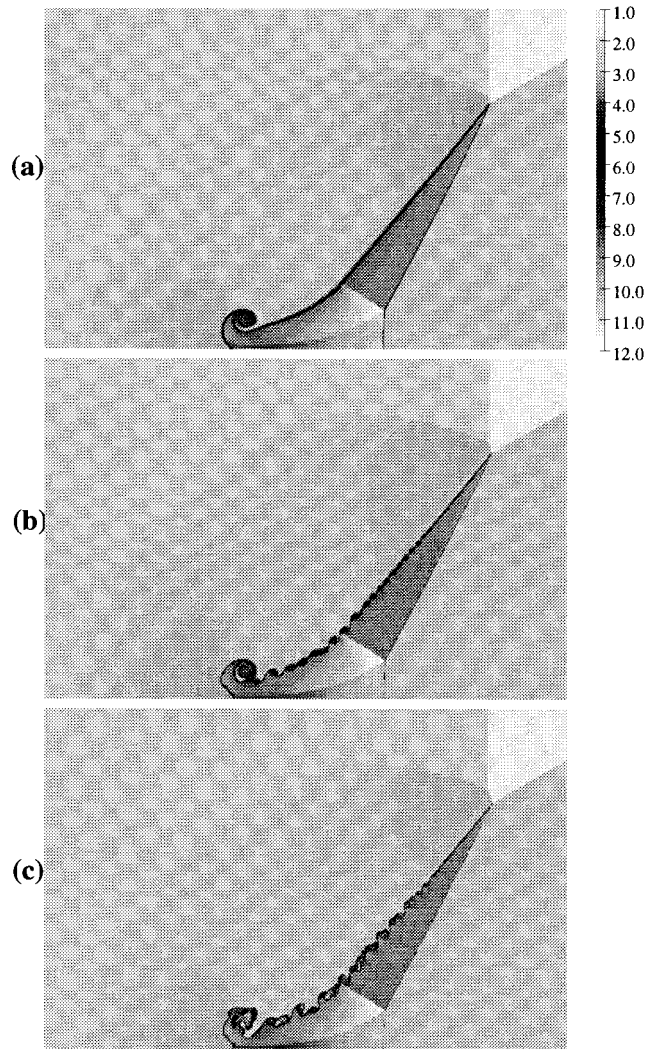


FIG. 2. Density images at $t=1$ for the shock refraction process solved as an initial-value problem. Grid sizes: (a) 768×392 , (b) 1536×768 , and (c) 3072×1536 .

changes in all scales equal to or smaller than the shear layer thickness. It is quite possible that the detailed shapes of the structures at given resolution are dependent on the numerical method including the specific slope limiter.

An attempt was made to test for weak convergence in the numerical sense¹⁵ by integration of the density (and velocity) weighted with a test function as follows:

$$\hat{\rho}(x,y,t) = \int \phi(x,y;x_0,y_0)\rho(x_0,y_0,t)dx_0 dy_0, \quad (3)$$

where the test function is given by

$$\phi(x,y;x_0,y_0) = \begin{cases} \left[1 + \cos\left(2\pi\frac{(x-x_0)}{\delta}\right) \right] \left[1 + \cos\left(2\pi\frac{(y-y_0)}{\delta}\right) \right] \delta^{-2}, & |x-x_0| \leq \frac{\delta}{2}, \quad |y-y_0| \leq \frac{\delta}{2}, \\ 0, & \text{otherwise.} \end{cases} \quad (4)$$

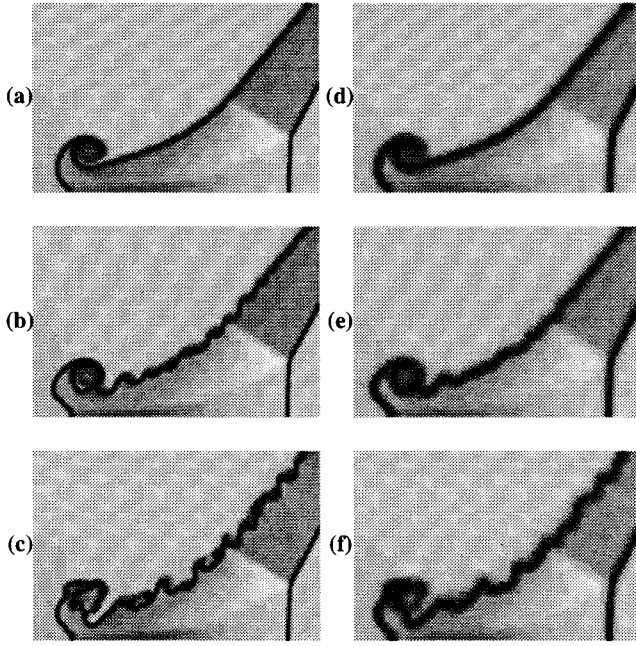


FIG. 3. Subdomain of the filtered density images at $t=1$ for the shock refraction process solved as an initial-value problem. Mesh spacing for: (a),(d) is h ; (b),(e) is $h/2$ and (c), (f) is $h/4$. For (a)–(c): $\delta=10h$, and (d)–(f): $\delta=20h$, where h is the mesh spacing for the 768×384 (coarse) mesh.

If $\delta=(\Delta x)^{1/2}$ then the above filtering process should remove any grid level oscillations. The smoothed fields showed no evidence of convergence. We next used $\delta=10h, 20h$ where h is the mesh spacing for the coarse mesh. The filtered density fields ($\hat{\rho}$) are shown in Fig. 3. We see no evidence of weak convergence when δ is held fixed and Δx is reduced. Moreover, the results for the two values of δ are not the same, implying dependence on δ .

The calculation for the fine grid was repeated in single precision arithmetic with no visual change in the contours of Fig. 2(c). A different numerical method, the kinetic-based equilibrium flux method (EFM)¹⁶ was also tried. This gave different looking contour plots at the same resolution. Our tentative conclusion is that there is no evidence of convergence to a method-independent solution, at fixed time, which has the property that the slip-line discontinuity resides on a rectifiable curve.

III. NUMERICAL SOLUTION OF THE SIMILARITY EQUATIONS

While the similarity structure of solutions to the unsteady multidimensional compressible Euler equations with appropriate boundary and initial conditions has long been recognized (see for example Refs. 17–19), all relevant numerical solutions known to us have been obtained by solving the initial-value problem. In this section, we outline a method to solve Eq. (2) numerically as a *boundary value problem*. The numerical method employed here is an *implicit* second order Godunov method. The discretized form of Eq. (2) (dropping the tilde over U , F and G) is

$$2U_{i,j}^{n+1} + \frac{F_{i+1/2,j}^{n+1} - F_{i-1/2,j}^{n+1}}{\Delta \xi_{i,j}} + \frac{G_{i,j+1/2}^{n+1} - G_{i,j-1/2}^{n+1}}{\Delta \eta_{i,j}} = 0, \quad (5)$$

where

$$F_{i+1/2,j}^{n+1} \equiv F(U_{L,i+1/2,j}^{n+1}, U_{R,i+1/2,j}^{n+1}), \quad (6)$$

$$F_{i+1/2,j}^{n+1} = F_{i+1/2,j}^n + \left(\frac{\partial F}{\partial U_L} \right)_{i+1/2,j}^n \delta U_{L,i+1/2,j}^n + \left(\frac{\partial F}{\partial U_R} \right)_{i+1/2,j}^n \delta U_{R,i+1/2,j}^n + \dots$$

The flux $G_{i,j+1/2}^{n+1}$ is expanded as a Taylor series in a similar manner. The fluxes at iteration n are evaluated by solving the Riemann problem with given left and right states $U_{L,i+1/2,j}^n, U_{R,i+1/2,j}^n$, respectively. Second order in (ξ, η) space is achieved in the same manner as for the initial-value problem. Substituting the Taylor series expansions for $F_{i\pm 1/2,j}^{n+1}$ and $G_{i,j\pm 1/2}^{n+1}$ in to Eq. (5) leads to a block pentadiagonal system

$$2\delta U_{i,j}^n + (A_{L,i+1/2,j}^n + A_{R,i-1/2,j}^n + B_{L,i,j+1/2}^n + B_{R,i,j-1/2}^n) \delta U_{i,j}^n + A_{L,i-1/2,j}^n \delta U_{i-1,j}^n + A_{R,i+1/2,j}^n \delta U_{i+1,j}^n + B_{L,i,j-1/2}^n \delta U_{i,j-1}^n + B_{R,i,j+1/2}^n \delta U_{i,j+1}^n = \mathcal{R}_{i,j}^n, \quad (7)$$

where $\delta U_{i,j}^n = U_{i,j}^{n+1} - U_{i,j}^n$ and

$$A_{K,i\pm 1/2,j} = \left(\frac{\partial F}{\partial U_K} \right)_{i\pm 1/2,j}, \quad B_{K,i,j\pm 1/2} = \left(\frac{\partial G}{\partial U_K} \right)_{i,j\pm 1/2}, \quad K=L,R \quad (8)$$

are the Jacobians of the fluxes F and G which are evaluated analytically by solving a linearly perturbed Riemann problem. Equation (7) is iterated until the L_∞ norm of the residual given by Eq. (9) is sufficiently small,

$$\|\mathcal{R}_{i,j}^n\| \equiv \sup \left(\left| 2U_{i,j}^n + \frac{F_{i+1/2,j}^n - F_{i-1/2,j}^n}{\Delta \xi_{i,j}} + \frac{G_{i,j+1/2}^n - G_{i,j-1/2}^n}{\Delta \eta_{i,j}} \right| \right) < \epsilon. \quad (9)$$

For a mesh size of $N \times M$, Eq. (7) may be expressed as

$$\mathcal{A}^n \delta U^n = \mathcal{R}^n. \quad (10)$$

where \mathcal{A} is a block pentadiagonal matrix of size $NM \times NM$ and each block is a 4×4 matrix, and the vector δU^n is a vector of NM unknowns. The bandwidth of \mathcal{A} is $8N+4$. For the larger of the mesh sizes given below, the bandwidth of \mathcal{A} is 12 292 and the number of unknowns is $NM \approx 4.72 \times 10^6$. Direct inversion of \mathcal{A} would produce a Newton–Raphson method but is not possible with current computational resources. We instead employ an alternating direction implicit (ADI) iterative technique to solve Eq. (10). For ease of parallel implementation \mathcal{A} is factored into two block tridiagonal matrices which are solved successively using a standard algorithm. The code was implemented on a

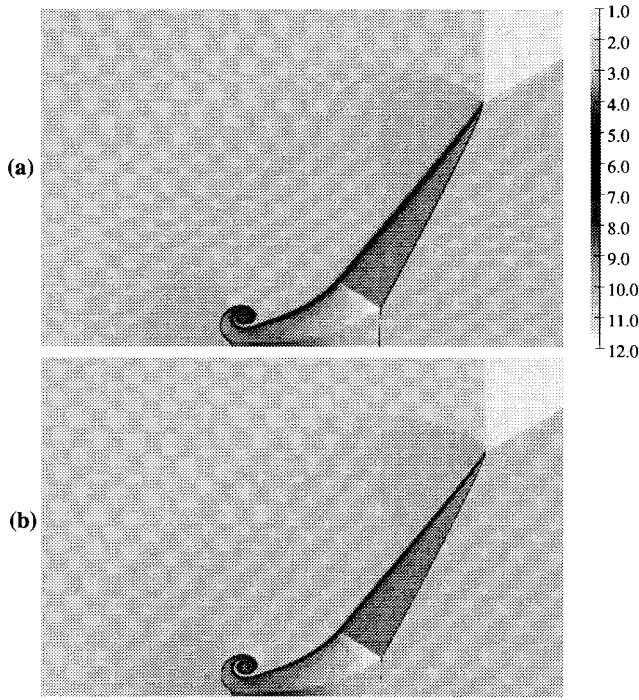


FIG. 4. Density images for self-similar solution of the shock refraction process solved as a boundary value problem. Grid sizes: (a) 768×392 and (b) 1536×768 .

message-passing 512 node Intel Paragon at Caltech. Gray scale images of density for grids of sizes (a) 768×392 and (b) 1536×768 are shown in Fig. 4. For the 1536×768 grid, the maximum norm of the residual for the continuity and the energy equation is plotted (Fig. 5) to demonstrate convergence to the fixed point of the discretization of Eq. (2). Further grid refinement for the self-similar problem was not feasible for the given computational resources. There appears to be pointwise convergence everywhere except in a thin region surrounding the slip-line discontinuity, and in the vicinity of the center of the rolled-up shear layer. The EFM was also tried for the self-similar problem. This produced densities (and other contour fields) which were nearly identical to

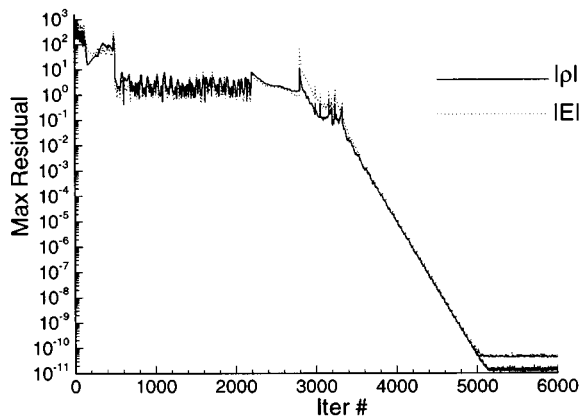


FIG. 5. Maximum residual for the continuity and the energy equation for the self-similar problem. The grid size is 1536×768 .

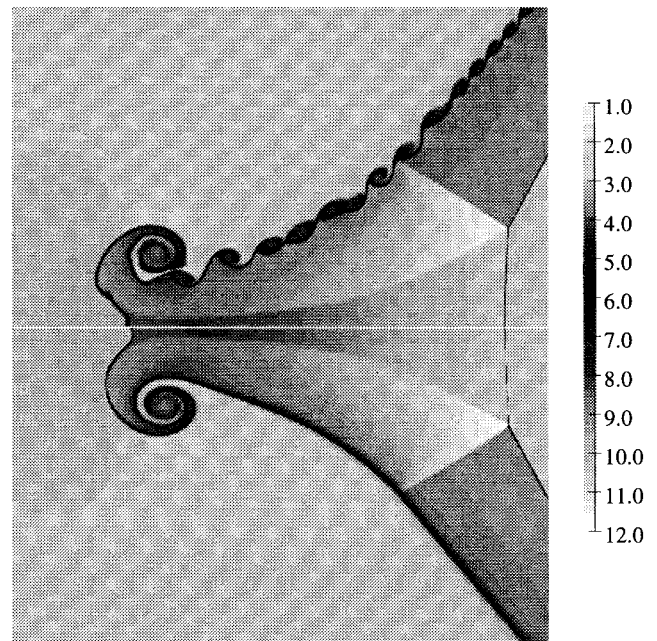


FIG. 6. A zoom of juxtaposition of the density for unsteady solution and the self-similar solution. The grid size is 1536×768 . The self-similar solution has been reflected about the ξ axis.

those of Fig. 3, at the same resolution, except near the center of roll-up. This is probably because at given resolution, the EFM is somewhat more numerically diffusive than the Godunov method. A zoom of the density is shown in Fig. 6 for the 1536×768 grid to compare and contrast the initial-value and the similarity approaches.

We define a self-similar Mach number as

$$\tilde{M}^2 = \frac{(\tilde{u}^2 + \tilde{v}^2)}{c^2}, \quad (11)$$

where $\tilde{u} = u - \xi$ and $\tilde{v} = v - \eta$, and $c^2 = \gamma p / \rho$ defines the sound speed. If $\tilde{M} < 1$ (≥ 1), then Eq. (2) is elliptic (hyperbolic). The contours of \tilde{M} are plotted in Fig. 7 with the dashed (solid) contours for subsonic (supersonic) \tilde{M} indicating regions of elliptic (hyperbolic) nature of the equations. Note that we have an elliptic region embedded in a hyperbolic one. The sufficient boundary conditions, comprising

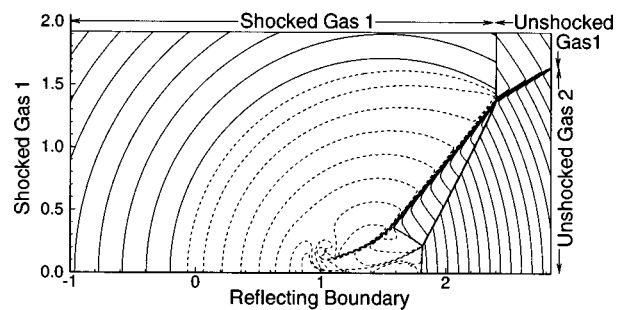


FIG. 7. Self similar Mach number, $\tilde{M} \in (0.0, 4.79)$. The subsonic contours are shown dashed. The sonic lines are the bounding dashed contours.

the shock speed and the location and slope of the contact discontinuity, are illustrated in Fig. 7. In principle, given the Cauchy boundary data one may march the solution in the hyperbolic region using the method of characteristics. However, this solution will terminate at one or more sonic lines. Since the location of the sonic lines are not known a priori, we clearly need to solve the system of equations as a boundary-value problem.

IV. CONCLUSION

For the mesh resolutions used presently, we find no evidence of either pointwise or of weak convergence in a neighborhood of the slip-line discontinuity, of our numerical solutions of the initial-value problem with $M_c < 1$. If it is assumed that, following Delort,⁵ there exists a (possibly unique) weak solution to the compressible Euler equations with vortex-sheet initial data and given boundary conditions, and further, that this solution has itself a vortex-sheet structure, then we can suggest several possibilities for the geometry of the contact: (a) the slip-line discontinuity is a rectifiable curve, i.e., a curve for which an arc length can be defined; (b) the slip-line is a rectifiable curve except on a set of measure zero, i.e., one can define an arc length everywhere except at a finite number of points where the curve may be the focus, for example, of a tightly wound double spiral; and (c) the slip line is a curve of fractal dimension D where $1 < D \leq 2$. If either (a) and (b) are true, then one would expect that, given a suitable numerical method, convergence to the appropriate weak solution should be achievable, at least for finite times. We cannot rule out the possibility that this is indeed the case, but that our numerical methodology is not up to the task. The scenario given by (c) provides a basis for understanding the grid and method sensitivity observed presently. If this state exists, or if the weak solution has a structure different from that of the vortex sheet, it seems to us unlikely that it could be computed by conventional finite-volume methods, even those that invoke AMR (adaptive mesh refinement). Computation of some averaged or smoothed state may of course be possible with more refined methods. This would pose a considerable challenge for computational fluid dynamics. Hyperfine grids may be irrelevant. We note that the above discussion assumes uniqueness.

In contrast, for the given mesh sizes, our solutions of the discretized version of the self-similar formulation appears to be converging. We speculate that in the limit $\Delta \xi \rightarrow 0, \Delta \eta \rightarrow 0$, the self-similar solution will converge to the weak solutions of the self-similar Euler equations [Eq. (2)], and that the slip line discontinuity will be a rectifiable curve except perhaps at a single point where the roll-up of the vortex sheet near the lower boundary may produce a spiral structure which may have an infinite arc length. It is surprising that the numerical method is apparently able to define the structure of the spiral with increasing grid resolution, without any user input. Thus, the similarity method may be said to be ‘spiral-capturing’ in addition to shock-capturing. The similarity solution is here interpreted to be the zero disturbance solution of the initial-value problem; it resides on an unstable

manifold in some function space. We do not suggest that it is an appropriate ‘averaged’ state for the initial-value problem, and in fact we suspect that it is not.

Our argument may be summarized as follows: we have Delort’s proof, under restrictions, for incompressible Euler flow with vortex-sheet initial data. Assume, by analogy, the existence of weak solutions for compressible flow with, in our case, spontaneous production of slip lines. It is of interest to ask if these weak solutions can be computed by standard methods for the multidimensional Euler equations? Owing to lack of convergence over a range of scales we tentatively conclude that convergence to the weak solution cannot be achieved, for arbitrary times, at least by our methods. We suspect that this is true for $M_c < 1$, which includes the incompressible case. The situation may be different for $M_c > 1$. The similarity problem is the initial-value problem in a restricted setting. We find evidence of convergence to a weak solution with a slip-line structure.

We accept the use of the initial-value problem for the multidimensional Euler equations (with embedded vortex sheets) as a model of real fluid behavior but suggest that the pursuit of ultra-high resolution with techniques like AMR may be futile. AMR methods are nevertheless useful since they can probably optimize the computational effort required to achieve a given local resolution.

ACKNOWLEDGMENTS

This work was supported in part by AFOSR Grant No. F49620-93-1-0338. Useful discussions with P. Dimotakis, T. Hou, D. I. Meiron and J. Quirk are gratefully acknowledged. This research was performed in part using the CSCC parallel computer system operated by Caltech on behalf of the Concurrent Supercomputing Consortium.

- ¹R. Krasny, “A study of singularity formation in a vortex sheet by the point vortex approximation,” *J. Fluid Mech.* **167**, 65 (1986).
- ²J. S. Ely and G. R. Baker, “High precision calculations of vortex sheet motion,” *J. Comput. Phys.* **111**, 275 (1994).
- ³P. R. Garabedian, *Partial Differential Equations* (Wiley, New York, 1964).
- ⁴D. W. Moore, “The spontaneous appearance of a singularity in the shape of an evolving vortex sheet,” *Proc. R. Soc. London A* **365**, 105 (1979).
- ⁵J.-M. Delort, “Existence de nappes de tourbillon en dimension deux,” *J. Am. Math. Soc.* **4**, 553 (1991).
- ⁶J. W. Miles, “On the disturbed motion of a plane vortex sheet,” *J. Fluid Mech.* **3**, 538 (1958).
- ⁷J. J. Quirk, “An alternative to unstructured grids for computing gas dynamic flows around arbitrarily complex two dimensional bodies,” *Comput. Fluids* **23**, 125 (1994).
- ⁸M. J. Berger and P. Colella, “Local adaptive mesh refinement for shock hydrodynamics,” *J. Comput. Phys.* **82**, 64 (1989).
- ⁹W. Mulder, S. Osher, and J. A. Sethian, “Computing interface motion in compressible gas dynamics,” *J. Comput. Phys.* **100**, 209 (1992).
- ¹⁰J. B. Bell, P. Colella, and H. M. Glaz, “A second order projection method for the incompressible Navier-Stokes equations,” *J. Comput. Phys.* **85**, 257 (1989).
- ¹¹H. G. Hornung, “Regular and Mach reflection of shock waves,” *Annu. Rev. Fluid Mech.* **18**, 33 (1986).
- ¹²S. K. Godunov, “Difference methods for the numerical solution of the equations of fluid dynamics,” *Mat. Sb.* **47**, 271 (1959).
- ¹³B. Van Leer, “Towards the ultimate conservative difference scheme IV: A new approach to numerical convection,” *J. Comput. Phys.* **23**, 276 (1977).
- ¹⁴R. Samtaney and N. J. Zabusky, “Circulation deposition on shock-accelerated planar and curved density-stratified interfaces: models and scaling laws,” *J. Fluid Mech.* **269**, 45 (1994).

¹⁵T. Hou (private communication, 1996).

¹⁶D. I. Pullin, "Direct simulation methods for compressible ideal gas flow," *J. Comput. Phys.* **34**, 231 (1980).

¹⁷L. F. Henderson, P. Colella, and E. G. Puckett, "On the refraction of shock waves at a slow-fast gas interface," *J. Fluid Mech.* **224**, 1 (1991).

¹⁸H. M. Glaz, P. Colella, I. I. Glass, and R. L. Deschambault, "A numerical study of shock-wave reflection with experimental comparisons," *Proc. R. Soc. London Ser. A* **398**, 117 (1985).

¹⁹P. Kutler and V. S. Vijaya Shankar, "Diffraction of a shock wave by a compression corner: I. Regular reflection," *AIAA J.* **15**, 197 (1977).